Reductive Elimination of Aryl Halides upon Addition of Hindered Alkylphosphines to Dimeric Arylpalladium(II) Halide Complexes

Amy H. Roy and John F. Hartwig*

Department of Chemistry, Yale University, P.O. Box 208107, New Haven, Connecticut 06520-8107

Received November 3, 2003

We report the reductive elimination of haloarene from $\{Pd[P(o\text{-tol})_3](Ar)(\mu\text{-X})\}_2$ (X = Cl, Br, I) upon addition of the strongly electron-donating, but sterically hindered, phosphine $P(t\text{-Bu})_3$ and related ligands. Reductive elimination of aryl chlorides, bromides, and iodides from these dimeric arylpalladium(II) halide complexes was observed upon the addition of $P(t\text{-Bu})_3$. Conditions to observe the elimination and addition equilibria were established for all three halides, and values for these equilibrium constants were measured. Reductive elimination of aryl chlorides was most favored thermodynamically, and elimination of aryl iodide was the least favored. However, reactions of the aryl chloride complexes were the slowest. Detailed mechanistic data revealed that cleavage of the starting dimer, accompanied by ligand substitution either before or after cleavage, led to the formation of a three-coordinate arylpalladium(II) halide monomer that reductively eliminated haloarene.

Introduction

The oxidative addition of aryl halides to palladium(0) complexes[1,2] is the initial step of catalytic processes such as Heck,[3−5] Stille,[6,7] Negishi,[8,9] and Suzuki coupling[10] as well as the recently developed arylation of amines,[11−14] ethers,[15,16] and carbonyl compounds.[17,18] A general catalytic cycle for these palladium-catalyzed reactions is shown in Scheme 1. Essentially any phosphine-ligated palladium(0) complex studied previously undergoes oxidative addition of aryl bromides and iodides. The opposite reaction, reductive elimination of haloarenes, is rare because addition is favored thermodynamically. A single example of haloarene reductive elimination was observed from a higher valent platinum(IV) species many years ago,[19] but reductive elimination from low-valent centers had not been observed directly until recently.[20]

Scheme 1

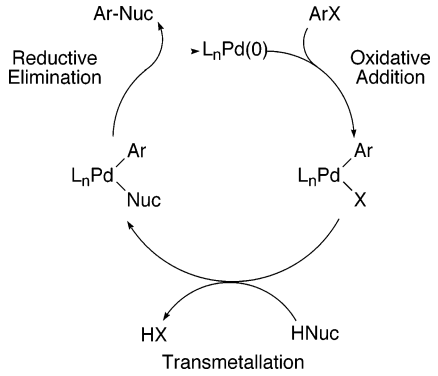

In general, complexes with increasingly electron-donating ligands undergo faster oxidative addition because of the greater driving force for oxidation of a more electron-rich metal.[21,22] Indeed, trialkylphosphine complexes add even chloroarenes,[23] and some of these and related ligands provide fast rates for coupling processes.[24] $P(t\text{-Bu})_3$ is the quintessential strongly electron donating ligand. Its ν_{CO} value for $\{Ni[P(t\text{-Bu})_3](CO)_3\}$ is the lowest of any phosphine ligand in Tolman's classic study.[25] Yet, we observed that reductive elimination of haloarene is induced by addition of tri-*tert*-butylphosphine to $\{Pd[P(o\text{-tol})_3](Ar)(\mu\text{-X})\}_2$ and is favored thermodynamically over oxidative addition. Thus, the steric properties of $P(t\text{-Bu})_3$ create the unusual thermodynamics for the addition and elimination equi-

* Corresponding author. E-mail: john.hartwig@yale.edu.

(1) Amatore, C.; Jutand, A. *J. Organomet. Chem.* **1999**, *573*, 254.
(2) Stille, J. K.; Lau, K. S. Y. *Acc. Chem. Res.* **1977**, *10*, 434.
(3) Heck, R. F. *Org. React.* **1982**, *27*, 345.
(4) Crisp, G. T. *Chem. Soc. Rev.* **1998**, *27*, 427.
(5) Beletskaya, I. P.; Cheprakov, A. V. *Chem. Rev.* **2000**, *100*, 3009.
(6) Stille, J. K. *Angew. Chem., Int. Ed. Engl.* **1986**, *25*, 508.
(7) Farina, V.; Krishnamurthy, V.; Scott, W. J. *Org. React.* **1997**, *50*, 1.
(8) Stanforth, S. P. *Tetrahedron* **1998**, *54*, 263.
(9) Negishi, E. *Handbook of Organopalladium Chemistry for Organic Synthesis*; John Wiley & Sons: New York, 2002; Vol. 1, p 229.
(10) Miyaura, N.; Suzuki, A. *Chem. Rev.* **1995**, *95*, 2457.
(11) Hartwig, J. F. *Angew. Chem., Int. Ed.* **1998**, *37*, 2046.
(12) Hartwig, J. F. In *Modern Amination Methods*; Ricci, A., Ed.; Wiley-VCH: Weinheim, 2000; p 195.
(13) Yang, B. H.; Buchwald, S. L. *J. Organomet. Chem.* **1999**, *576*, 125.
(14) Wolfe, J. P.; Wagaw, S.; Marcoux, J.-F.; Buchwald, S. L. *Acc. Chem. Res.* **1998**, *31*, 805.
(15) Mann, G.; Incarvito, C.; Rheingold, A. L.; Hartwig, J. F. *J. Am. Chem. Soc.* **1999**, *121*, 3224.
(16) Aranyos, A.; Old, D. W.; Kiyomori, A.; Wolfe, J. P.; Sadighi, J. P.; Buchwald, S. L. *J. Am. Chem. Soc.* **1999**, *121*, 4369.
(17) Kawatsura, M.; Hartwig, J. F. *J. Am. Chem. Soc.* **1999**, *121*, 1473.
(18) Fox, J. M.; Huang, X.; Chieffi, A.; Buchwald, S. L. *J. Am. Chem. Soc.* **2000**, *122*, 1360.
(19) Ettorre, R. *Inorg. Nucl. Chem. Lett.* **1969**, *5*, 45.
(20) Roy, A. H.; Hartwig, J. F. *J. Am. Chem. Soc.* **2003**, *125*, 13944.
(21) Collman, J. P.; Hegedus, L. S.; Norton, J. R.; Finke, R. G. *Principles and Applications of Organotransition Metal Chemistry*, 2nd ed.; University Science Books: Mill Valley, CA, 1987.
(22) Crabtree, R. H. *The Organometallic Chemistry of the Transition Metals*, 3rd ed.; John Wiley & Sons: New York, 2001.
(23) Portnoy, M.; Milstein, D. *Organometallics* **1993**, *12*, 1665.
(24) Littke, A. F.; Fu, G. C. *Angew. Chem., Int. Ed.* **2002**, *41*, 4176.
(25) Tolman, C. A. *Chem. Rev.* **1977**, *77*, 313.

10.1021/om034277u CCC: $27.50
Publication on Web 02/25/2004

Scheme 2

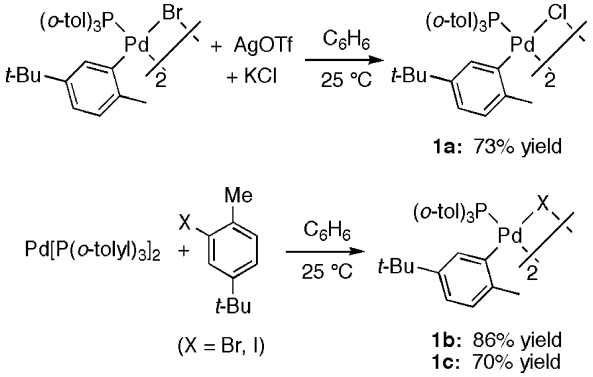

librium. We provide equilibrium constants for these addition and elimination processes.

Recently, P(*t*-Bu)$_3$-ligated arylpalladium halide complexes[26] have been isolated and fully characterized. The availability of spectral data for these complexes now allows a clear determination of whether P(*t*-Bu)$_3$-ligated complexes are present during the reactions of {Pd[P(*o*-tol)$_3$](Ar)(μ-X)}$_2$ with P(*t*-Bu)$_3$. Detailed kinetic studies on the reductive elimination of bromoarene and chloroarene and the accumulation of reaction intermediates during these reactions are now reported along with simulation of kinetic data. These results reveal that an equilibrium comprised of dimer cleavage and ligand substitution leads to the formation of monomeric three-coordinate, P(*t*-Bu)$_3$-ligated arylpalladium(II) halide complexes prior to a slower reductive elimination of bromo- and chloroarene.

Results

Synthesis of {Pd[P(*o*-tolyl)$_3$](Ar)(μ-X)}$_2$ (1a−e). Compounds **1a**−**c** were synthesized as shown in Scheme 2. Reaction of {Pd[P(*o*-tolyl)$_3$](2-Me-5-*t*-Bu-C$_6$H$_3$)(μ-Br)}$_2$ with AgOTf and KCl at room temperature produced {Pd[P(*o*-tolyl)$_3$](2-Me-5-*t*-Bu-C$_6$H$_3$)(μ-Cl)}$_2$ (**1a**) in 73% yield. Oxidative addition of 2-bromo-4-*tert*-butyltoluene or 2-iodo-4-*tert*-butyltoluene to Pd[P(*o*-tolyl)$_3$]$_2$ at room temperature formed {Pd[P(*o*-tolyl)$_3$](2-Me-5-*t*-Bu-C$_6$H$_3$)(μ-Br)}$_2$ (**1b**) and {Pd[P(*o*-tolyl)$_3$](2-Me-5-*t*-Bu-C$_6$H$_3$)(μ-I)}$_2$ (**1c**) in 86% and 70% yields. Compounds **1d** and **1e** (Ar = *t*-BuC$_6$H$_4$, eq 1) were prepared by literature procedures.[27]

Reductive Elimination of Haloarene from {Pd[P(*o*-tol)$_3$](Ar)(μ-X)}$_2$. Compounds **1a**−**e** underwent reductive elimination upon addition of P(*t*-Bu)$_3$ and heating at 70 °C. These reductive elimination processes produced a 30−75% yield of haloarene. Equation 1 and Table 1 summarize the data on the reductive elimination of haloarene from complexes **1a**−**e** upon addition of P(*t*-Bu)$_3$. Complexes with *t*-Bu substituents on the palladium-bound aryl group were studied to ensure high solubility of the dimeric reactants in arene solvents. All of the P(*o*-tolyl)$_3$-ligated arylpalladium halide complexes formed {Pd[P(*t*-Bu)$_3$]$_2$} (**2**)[28] upon addition of an excess of P(*t*-Bu)$_3$. Complex **1a** with an ortho-substituted palladium-bound aryl group provided higher yields of free chloroarene product than did complex **1d**, containing an unhindered palladium-bound aryl group. Biaryl was the predominant side product. The amount of added P(*t*-Bu)$_3$ was crucial to obtain high yields of free haloarene. The highest yields were obtained when approximately 15 equiv of P(*t*-Bu)$_3$ per dimer was used.

Table 1. Yield of ArX and the Calculated K_{eq}[a] Value for the Reductive Elimination of Haloarene from {Pd[P(*o*-tolyl)$_3$](Ar)(X)}$_2$

X	yield of ArX (%)	K_{eq}
Ar = 2-Me-5-*t*-BuC$_6$H$_3$		
1a (X = Cl)	70	$9(3) \times 10^{-2}$
1b (X = Br)	70	$2.3(3) \times 10^{-3}$
1c (X = I)	39	$3.7(2) \times 10^{-5}$
Ar = 4-*t*-BuC$_6$H$_4$		
1d (X = Cl,)	30	not measured[b]
1e (X = Br)	75	$3.3(6) \times 10^{-4}$

[a] K_{eq} values are referenced to a 1 M standard state. [b] This reaction appeared to consume all of the chloroarene complex, but low yields for the formation of free aryl chloride may prevent reversibility.

K_{eq} values (Table 1) were obtained for the process in eq 1 by initiating reactions in both directions. Qualitatively, an equilibrium was established when less than 4 equiv of P(*t*-Bu)$_3$ was added to a 10 mM solution of chloride **1a**, less than 10 equiv to a 10 mM solution of bromide **1b**, and less than 15 equiv to the same solution of iodide **1c**. Quantitative data are provided in Table 1. An ortho methyl group on the haloarene increased the value of K_{eq} for reductive elimination by a factor of roughly 10. Chloride **1a** displayed the largest driving force for reductive elimination, and iodide **1c** had the smallest. The change in K_{eq} that accompanied each successive change of halide was roughly a factor of 100.

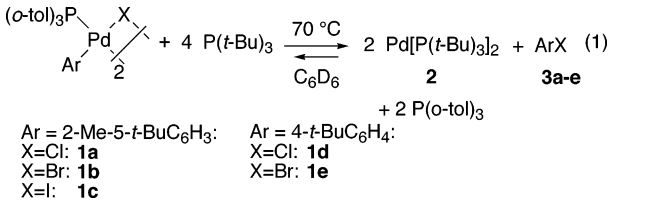

The reductive elimination of haloarene from arylpalladium halide complexes also occurred upon addition of bulky phosphine ligands other than P(*t*-Bu)$_3$. Scheme 3 summarizes the data for the reductive elimination of haloarene from complexes **1a**−**c** upon addition of various ligands. Reaction between complexes **1a**−**c** and (biphenyl)di-*tert*-butylphosphine, ferrocenyldi-*tert*-butylphosphine, or the unsaturated diisopropyl *N*-heterocyclic carbene ligand consumed the starting P(*o*-tol)$_3$ complex, but did not produce haloarene. However, reaction between **1a** or **1b** and PCy(*t*-Bu)$_2$ formed haloarene in 10−15% yield, while reaction of **1a** or **1b** with 1-adamantyl-di-*tert*-butylphosphine (1-AdP(*t*-Bu)$_2$) and 1,2,3,4,5-pentaphenyl-1′-(di-*tert*-butylphosphino)-ferrocene (Q-phos) produced haloarene in 69−81% yields and 42−52% yields, respectively.

Observation of Pd[P(*t*-Bu)$_3$](2-Me-5-*t*-Bu-C$_6$H$_3$)(Br) in the Reductive Elimination of Haloarene from {Pd[P(*o*-tolyl)$_3$](2-Me-5-*t*-Bu-C$_6$H$_3$)(Br)}$_2$. During our previous work on the reductive elimination of haloarene from {Pd[P(*o*-tolyl)$_3$](2-Me-5-*t*-Bu-C$_6$H$_3$)(Br)}$_2$, we postulated that the reductive elimination occurred

(26) Stambuli, J. P.; Buhl, M.; Hartwig, J. F. *J. Am. Chem. Soc.* **2002**, *124*, 9346.
(27) Paul, F.; Patt, J.; Hartwig, J. F. *Organometallics* **1995**, *14*, 3030.
(28) Yoshida, T.; Otsuka, S. *J. Am. Chem. Soc.* **1977**, *99*, 2134.

Scheme 3

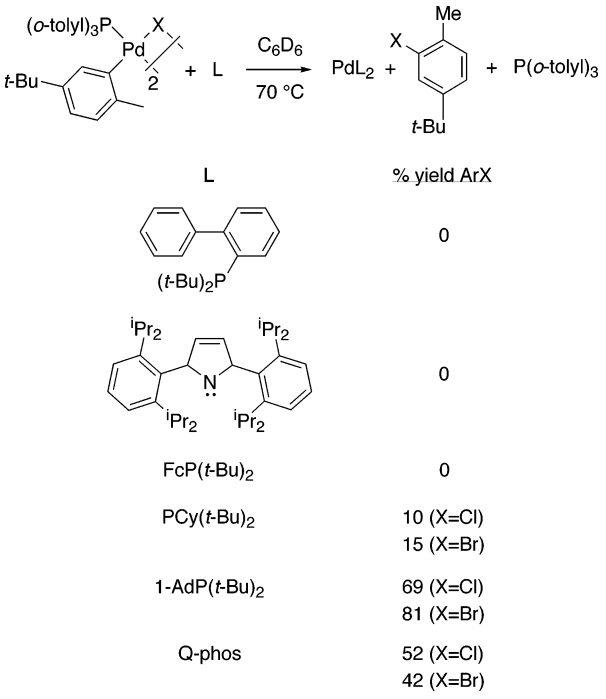

from a three-coordinate arylpalladium halide intermediate ligated by P(*t*-Bu)$_3$.[29] We did not observe this intermediate during the reductive elimination due to its low concentration, broad *tert*-butyl resonance in the ^{1}H NMR spectrum, and a ^{31}P NMR chemical shift that was nearly identical to that of free P(*t*-Bu)$_3$.

Recently, three-coordinate arylpalladium(II) halide monomers ligated by P(*t*-Bu)$_3$ or 1-AdP(*t*-Bu)$_2$ were isolated and characterized.[26] We attempted to prepare Pd[P(*t*-Bu)$_3$](2-Me-5-*t*-Bu-C$_6$H$_3$)(Br) (**4**), which would be the actual intermediate formed by cleavage of the dimeric P(*o*-tol)$_3$ complex and substitution of P(*t*-Bu)$_3$ for the phosphine in {Pd[P(*o*-tolyl)$_3$](2-Me-5-*t*-Bu-C$_6$H$_3$)(Br)}$_2$, but complex **4** was not stable enough in solution under the reaction conditions to isolate in pure form.

Instead, Pd[P(*t*-Bu)$_3$](*o*-tolyl)(Br) was synthesized and characterized, as recently reported.[20] With the spectral features of this similar complex, we identified the *tert*-butyl and tolyl signals of Pd[P(*t*-Bu)$_3$](2-Me-5-*t*-Bu-C$_6$H$_3$)(Br) in the ^{1}H NMR spectra obtained during the reactions of {Pd[P(*o*-tolyl)$_3$](2-Me-5-*t*-Bu-C$_6$H$_3$)(Br)}$_2$ with P(*t*-Bu)$_3$ that led to reductive elimination of haloarene. Complex **4** accumulated in approximately 11% yield after heating of a solution of 0.013 M {Pd[P(*o*-tolyl)$_3$](2-Me-5-*t*-Bu-C$_6$H$_3$)(Br)}$_2$ and 0.068 M P(*t*-Bu)$_3$ for 10 min at 70 °C.

Because the ^{31}P NMR chemical shift of the arylpalladium complexes ligated by (1-Ad)P(*t*-Bu)$_2$ is more clearly resolved from the shift of free (1-Ad)P(*t*-Bu)$_2$, we conducted the reaction of {Pd[P(*o*-tolyl)$_3$](2-Me-5-*t*-Bu-C$_6$H$_3$)(Br)}$_2$ with (1-Ad)P(*t*-Bu)$_2$ at 70 °C and evaluated the presence or absence of accumulated Pd[(1-Ad)P(*t*-Bu)$_2$](2-Me-5-*t*-Bu-C$_6$H$_3$)(Br) by ^{1}H and ^{31}P NMR spectroscopy. Indeed, approximately 12% of Pd[1-AdP(*t*-Bu)$_2$](2-Me-5-*t*-Bu-C$_6$H$_3$)(Br) was observed clearly after 2 h during the reaction between 0.011 M {Pd[P(*o*-tolyl)$_3$]-(2-Me-5-*t*-Bu-C$_6$H$_3$)(Br)}$_2$ and 0.051 M 1-AdP(*t*-Bu)$_2$ at 70 °C.

(29) Roy, A. H.; Hartwig, J. F. *J. Am. Chem. Soc.* **2001**, 1232.

Table 2. Dependence of k_{obs} on [1b]$_o$ from Fits to Half-Order and First-Order Appearance of Product

[**1b**]$_o$ (M)	k_{obs} ($M^{1/2}$ s^{-1})	k_{obs} (s^{-1})
0.518×10^{-2}	2.91×10^{-5}	1.42×10^{-4}
1.02×10^{-2}	2.78×10^{-5}	1.07×10^{-4}
2.05×10^{-2}	3.07×10^{-5}	0.88×10^{-4}

Mechanism of Reductive Elimination of Haloarenes from {Pd[P(*o*-tolyl)$_3$](Ar)(X)}$_2$. The observation of Pd[P(*t*-Bu)$_3$](2-Me-5-*t*-Bu-C$_6$H$_3$)(Br) and Pd[(1-Ad)P(*t*-Bu)$_2$](2-Me-5-*t*-Bu-C$_6$H$_3$)(Br) during the reaction of {Pd[P(*o*-tolyl)$_3$](2-Me-5-*t*-Bu-C$_6$H$_3$)(Br)}$_2$ with P(*t*-Bu)$_3$ or (1-Ad)P(*t*-Bu)$_2$ suggests that reductive elimination from the monomeric arylpalladium(II) halide complexes was the rate-determining step. To substantiate this proposal, we measured the rate constants for reductive elimination of haloarene from chloride and bromide complexes **1a** and **1b** by ^{1}H NMR spectroscopy at 55 or 65 °C.

Kinetic Studies on the Reductive Elimination of Aryl Bromide from Arylpalladium Bromide 1b. Rate constants for the reaction in eq 2 were measured by ^{1}H NMR spectroscopy at 55 °C. The concentration of P(*t*-Bu)$_3$ was varied from 0.10 to 0.84 M. [P(*o*-tol)$_3$] was varied from 0.030 to 0.35 M, and [**1b**] was varied from 5.2 to 21 mM. Because P(*o*-tol)$_3$ may be generated reversibly during some steps of the reaction, the values of k_{obs} may depend on the concentration of P(*o*-tolyl)$_3$. Therefore, excess P(*o*-tolyl)$_3$ was added to the reactions to maintain a constant concentration. Excellent fits to both a first-order and a half-order appearance of product were obtained.

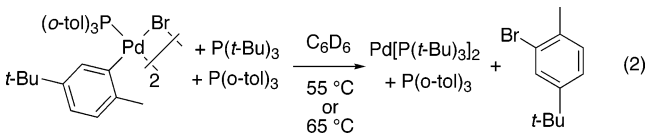

(2)

We had previously concluded that the reaction showed a first-order dependence on [**1b**].[29] However, additional values of k_{obs} obtained with varied initial concentrations of **1b** summarized in Table 2 have shown that the reaction most likely occurs with a half-order dependence on the concentration of **1b**. The values of k_{obs} obtained from fits to a half-order appearance of Pd[P(*t*-Bu)$_3$]$_2$ with reactions of varied initial concentrations of **1b** were indistinguishable. In contrast, the values of k_{obs} obtained from fits to a first-order appearance of Pd[P(*t*-Bu)$_3$]$_2$ with varied initial concentrations of **1b** were different.

Figure 1 shows the dependence of k_{obs} on the concentration of the two phosphines. A linear dependence of $1/k_{obs}$ on 1/[P(*t*-Bu)$_3$] was observed, along with a nonzero *y*-intercept. A linear dependence of k_{obs} on [P(*o*-tolyl)$_3$] was also observed, along with a nonzero *y*-intercept.

Qualitative mechanistic studies showed that the reaction was not affected by light and that anthracene was not formed as product when the reactions were run in the presence of 9,10-dihydroanthracene. Moreover, the rate constants were highly reproducible. Thus,

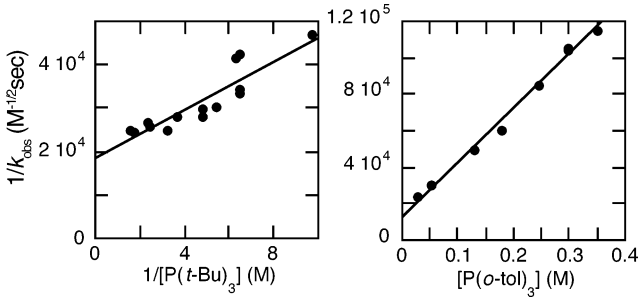

Figure 1. Plots of $1/k_{obs}$ vs $1/[P(t\text{-Bu})_3]$ and $1/k_{obs}$ vs $[P(o\text{-tol})_3]$ for the reductive elimination of aryl bromide from complex **1b** at 55 °C.

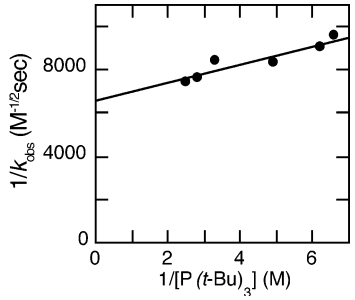

Figure 2. Plot of $1/k_{obs}$ vs $1/[P(t\text{-Bu})_3]$ for the reductive elimination of aryl bromide from **1b** at 65 °C.

further studies to detect a radical pathway were not conducted.

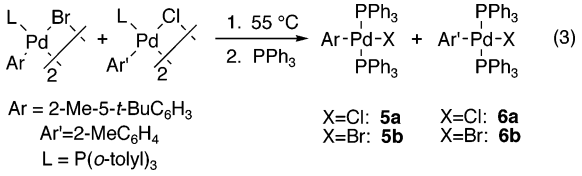

To probe for reversible cleavage of the dimer during the reductive elimination, we conducted the reaction in eq 3. A solution of two dimeric arylpalladium halide complexes, each with a different halide and aryl group, was heated at 55 °C. PPh_3 was added to the solution after 10 min to simplify the product distribution. Reversible cleavage of the dimers would form Pd[P(*o*-tolyl)$_3$](Ar)(X) that could recombine to form either dimer. This recombination would form three different dimers, which upon reaction with added PPh_3 would form complexes **5a**,**b** and **6a**,**b** in eq 3. If cleavage of the dimers had not occurred reversibly, addition of PPh_3 would form only **5b** and **6a**. The observation of four different $(PPh_3)_2$Pd(Ar)(X) complexes by NMR spectroscopy indicated that reversible cleavage of dimer had occurred after 10 min at 55 °C. Although several potential pathways for exchange are possible, this experiment was consistent with our expectation that cleavage of the halogen bridges is more rapid than the overall reaction at 55 °C.

To probe for reversible reductive elimination in the absence of added $P(t\text{-Bu})_3$, we added 4-BrC_6H_4-*t*-Bu to bromide complex **1b** and to {Pd[P(*o*-tolyl)$_3$](*p*-tol)(Br)}$_2$. Reversible reductive elimination would generate three different dinuclear complexes {Pd_2[P(*o*-tolyl)$_3$]$_2$(X)$_2$(Ar)(Ar′)}. However, only small amounts of exchange were observed after days at 55 °C; nearly all of **1b** and {Pd[P(*o*-tolyl)$_3$](*p*-tol)(Br)}$_2$ remained unreacted on the time scale of the reductive elimination. This result indicates that reductive elimination of haloarene does not occur directly from P(*o*-tolyl)$_3$-ligated arylpalladium complexes under the conditions of reductive elimination in the presence of added $P(t\text{-Bu})_3$.

The reductive elimination of chloroarene from chloride complex **1a** was slow at 55 °C and was studied at 65 °C instead. These results are discussed in the next section. To compare directly our data on the reductive elimination of bromoarene with data on the reductive elimination of chloroarene, rate constants for the reductive elimination of bromoarene from **1b** were also measured

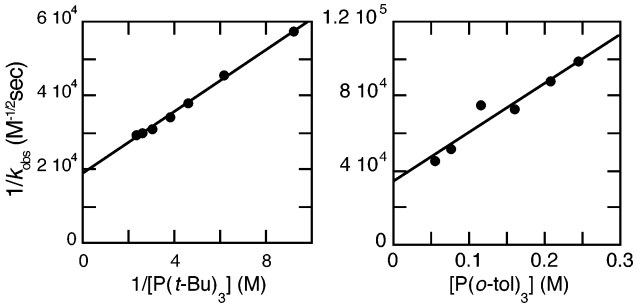

Figure 3. Plots of $1/k_{obs}$ vs $1/[P(t\text{-Bu})_3]$ and $1/k_{obs}$ vs $[P(o\text{-tol})_3]$ for the reductive elimination of aryl chloride from complex **1a** at 65 °C.

Table 3. Dependence of k_{obs} on $[1a]_o$ from Fits to Half-Order and First-Order Appearance of Product

$[1a]_o$ (M)	k_{obs} ($M^{1/2}$ s^{-1})	k_{obs} (s^{-1})
0.518×10^{-2}	1.52×10^{-3}	1.28×10^{-4}
2.05×10^{-2}	1.76×10^{-3}	6.65×10^{-5}

by ^{1}H NMR spectroscopy at 65 °C. The concentration of $P(t\text{-Bu})_3$ was varied from 0.15 to 0.51 M. Again, P(*o*-tol)$_3$ was added to the reactions to maintain a constant concentration. Excellent fits to a half-order appearance of each product were obtained. Figure 2 shows the dependence of k_{obs} on the concentration of $P(t\text{-Bu})_3$. A positive, linear dependence of $1/k_{obs}$ versus $1/[P(t\text{-Bu})_3]$ was observed, along with a nonzero *y*-intercept.

Kinetic Studies on the Reductive Elimination of Chloroarene from Arylpalladium Chloride Complex 1a. Rate constants for the reductive elimination of chloroarene from **1a** were measured by ^{1}H NMR spectroscopy at 65 °C. The concentration of $P(t\text{-Bu})_3$ was varied from 0.16 to 0.44 M, and $[P(o\text{-tol})_3]$ was varied from 0.054 to 0.25 M. Excess P(*o*-tolyl)$_3$ was again added to the reactions to maintain a constant concentration. Excellent fits to a half-order appearance of product were obtained. Although good fits to a first-order appearance of product were also observed, the data in Table 3 show that the reaction appears to be closer to half-order in the concentration of **1a** than first-order. The rate constants from a fit of the data to a first-order appearance of product depended on the initial concentration of **1a**, but rate constants from a fit of the data to a half-order appearance of product did not.

Figure 3 shows the dependence of k_{obs} on the concentration of the two phosphines. These results parallel the results on the reductive elimination of bromoarene upon addition of $P(t\text{-Bu})_3$ to **1b**. A linear dependence of $1/k_{obs}$ on $1/[P(t\text{-Bu})_3]$ was observed, along with a nonzero

Table 4. Ph−X Bond Strengths for X = Cl, Br, I[30]

X	Ph−X bond strength (kcal/mol)
Cl	96
Br	81
I	65

y-intercept. A linear dependence of $1/k_{obs}$ on [P(*o*-tolyl)$_3$] was also observed, along with a nonzero *y*-intercept.

Discussion

Reductive Elimination of Haloarene from {Pd[P(*o*-tolyl)$_3$](Ar)(μ-X)}$_2$. 1. Thermodynamic Considerations. Data on the yields of haloarene and on the values of K_{eq} for the reductive elimination of haloarene from {Pd[P(*o*-tolyl)$_3$](Ar)(μ-X)}$_2$ are summarized in Table 1. In the presence of 15 equiv of P(*t*-Bu)$_3$, the reductive elimination occurred to greater than 95% conversion of the starting palladium complex. Thus, the values of K_{eq} did not significantly limit reaction yields. The yields of haloarene and Pd(0) by the reductive elimination induced by addition of P(*t*-Bu)$_3$ to compounds **1a**−**c** paralleled the thermodynamic driving force, as shown in Table 4. Because the driving force for reductive elimination of iodoarene is weaker than that for elimination of bromoarene, reductive elimination from iodide **1c** required more added ligand for the reaction to occur to completion than did the reductive elimination from bromide **1b**. The yield of iodoarene produced from **1c** was also lower than the yield of bromoarene produced by reductive elimination from **1b** due to the formation of larger amounts of biaryl and arene. This trend in rates and yields parallels that observed for reductive elimination directly from [(*t*-Bu$_3$P)Pd(Ph)(X)] (X = I, Br).[20] The smaller driving force for formation of haloarene from **1c** than from **1b** indicates that the difference in energy between the carbon−bromine and carbon−iodine bonds is larger than the difference in energy between the palladium−bromine and palladium−iodine bonds.

However, reductive elimination of chloroarene from chloride complex **1a** required less P(*t*-Bu)$_3$ to push the reaction to completion than did the reductive elimination of bromoarene from **1b**. Thus, reductive elimination of chloroarene displays a greater driving force than elimination of the other haloarenes, and this greater driving force originates in the stronger C−Cl bond.

2. Kinetic Considerations. The rates of reductive elimination of haloarene from {Pd[P(*o*-tolyl)$_3$](Ar)(μ-X)}$_2$ did not parallel the thermodynamic driving force. Reductive elimination from chloride **1a** was slower than from bromide **1b**, even though reductive elimination from **1a** was more favored thermodynamically. The low yield of chloroarene from reaction of para-substituted **1d** is consistent with the slow rates for reaction of the more hindered chloride **1a**.

This comparison of rates of reaction of **1a** and **1b** shows that the relative rates for reaction of chloro- and bromoarenes are controlled by transition state energies, not by ground state thermodynamics. If the thermodynamic driving forces for the addition and elimination of haloarenes were to account for the differences in rates of reactions involving chloro-, bromo-, and iodoarenes, the elimination of chloroarene would be fastest. If differences in transition state energies were larger than differences in ground state energies, then the haloarene that generally adds the slowest would also eliminate the slowest. Because we observed the largest driving force but slowest elimination from the chloroarene, the slow rate for addition of chloroarenes cannot be attributed to the high C−X bond strength.

Instead, the relative reaction rates are more likely controlled by the ability of the intact haloarene to coordinate to the metal or to the electronic properties of the haloarene in the transition state for C−X bond formation and cleavage. If a haloarene complex with the halogen coordinated to the metal center is an intermediate in the addition and elimination process, then the stability of this intermediate may affect the transition state energy for the elimination and addition processes. Iodo- and bromoarene complexes are more stable than chloroarene complexes,[31] and this greater stability of the iodo- and bromoarene complexes could, therefore, account for the differences in reaction rates. Alternatively, the electronic properties of the halogen, such as softness, polarizability, or nucleophilicity, could control the rate of addition and elimination. The higher polarizability of bromide and iodide and greater electron-donating ability of these halogens may lead to a less polarized transition state and faster reductive elimination.

Computational studies on the pathway of the Heck reaction have evaluated the mechanism for oxidative addition of bromoarenes.[32] These studies suggested that a haloarene complex is an intermediate, but that the haloarene complex on the reaction pathway is an η^2-arene complex with the π-system of the haloarene coordinated to the metal, not an η^1-complex with the halogen coordinated to the metal. If so, then the electronic properties of the halogen would more likely influence the rate of addition and elimination than the rate and thermodynamics of coordination of the haloarene to the metal.

Mechanistic Studies on the Reductive Elimination of Haloarene from {Pd[P(*o*-tol)$_3$](Ar)(μ-X)}$_2$. The recent isolation of P(*t*-Bu)$_3$-ligated arylpalladium(II) halide monomers[26] allowed us to detect directly by ^{1}H NMR spectroscopy an accumulation of [P(*t*-Bu)$_3$]Pd(Ar)(Br) complexes during the reductive elimination of haloarene from bromide complex **1b**. In light of this observation, the proposal that ligand substitution is the rate-limiting step during the reaction of **1b** with P(*t*-Bu)$_3$ was reevaluated.[29]

Five classes of mechanism for the reductive elimination were considered, as shown in Schemes 4 and 5. Path A consists of an irreversible dissociative ligand substitution, followed by cleavage of the dinuclear species prior to reductive elimination as seen in eqs 4−6. The rate equation for dissociative substitution predicts positive slopes and nonzero *y*-intercepts for both plots in Figure 1. These predictions are consistent with the data in Figure 1. However, this mechanism also predicts first-order, rather than half-order, rate behavior in [**1b**] and a lack of accumulation of the three-coordinate

(30) Grushin, V. V.; Alper, H. *Chem. Rev.* **1994**, *94*, 7.
(31) Widenhoefer, R.; Buchwald, S. L. *Organometallics* **1996**, *15*, 2755.
(32) Sundermann, A.; Uzan, O.; Martin, J. M. L. *Chem. Eur. J.* **2001**, *7*, 1703.

Scheme 4

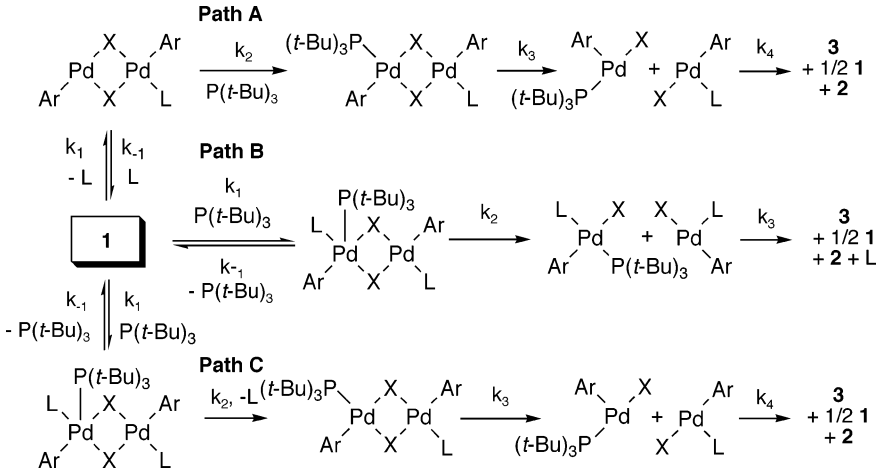

Scheme 5

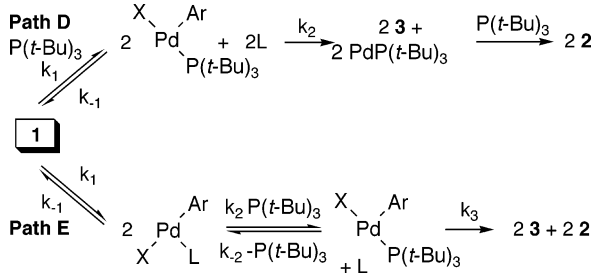

P(*t*-Bu)$_3$-ligated intermediate, **4**. These predictions are inconsistent with our data.

$$\text{rate} = k_{obs}[\mathbf{1b}] \tag{4}$$

$$k_{obs} = \frac{k_1 k_2[\text{P}(t\text{-Bu})_3]}{k_{-1}[\text{P}(o\text{-tol})_3] + k_2[\text{P}(t\text{-Bu})_3]} \tag{5}$$

$$\frac{1}{k_{obs}} = \frac{k_{-1}[\text{P}(o\text{-tol})_3]}{k_1 k_2[\text{P}(t\text{-Bu})_3]} + \frac{1}{k_1} \tag{6}$$

Path B involves initial coordination of P(*t*-Bu)$_3$ to palladium and either reversible or irreversible formation of a three-coordinate P(*o*-tol)$_3$ complex and a four-coordinate mixed phosphine complex. The four-coordinate, P(*t*-Bu)$_3$-ligated complex would then reductively eliminate haloarene either before or after dissociation of P(*o*-tolyl)$_3$. As shown in eqs 7 and 8, the rate equation for this associative mechanism with reversible formation of mononuclear species predicts a half-order dependence of the rate on [P(*t*-Bu)$_3$]. This prediction is inconsistent with the data in Figure 1, which shows a linear relationship between $1/k_{obs}$ and 1/[P(*t*-Bu)$_3$] and a nonzero *y*-intercept. This mechanism also predicts an absence of observable quantities of [P(*t*-Bu)$_3$]Pd(Ar)(Br). This prediction is again inconsistent with the direct observation of intermediate **4**. A version of path B in which association of P(*t*-Bu)$_3$ or cleavage of the dimer is irreversible would provide zero-order behavior in P(*o*-tolyl)$_3$ and no accumulation of intermediate **4**. Eq 9 shows a first-order dependence on [P(*t*-Bu)$_3$] and [**1b**] for the modified path B involving irreversible association of P(*t*-Bu)$_3$. The nonzero *y*-intercept, the inverse dependence of k_{obs} on [P(*o*-tolyl)$_3$] shown in Figure 1, and the observation of the P(*t*-Bu)$_3$-ligated intermediate are clearly inconsistent with predicted rate behavior for this modified path B.

$$\text{rate} = k_{obs}[\mathbf{1b}]^{1/2} \tag{7}$$

$$k_{obs} = K_1^{1/2} K_2^{1/2} k_3[\text{P}(t\text{-Bu})_3]^{1/2} \tag{8}$$

$$\text{rate} = k_1[\text{P}(t\text{-Bu})_3][\mathbf{1b}] \tag{9}$$

Path C shows an initial, reversible associative replacement of P(*t*-Bu)$_3$ for P(*o*-tolyl)$_3$ and irreversible cleavage of the resulting dinuclear species. As shown by rate equations 10−11, this mechanism would show a first-order dependence on [**1b**], a simple first-order dependence on [P(*t*-Bu)$_3$], an inverse dependence on [P(*o*-tolyl)$_3$], and a lack of accumulation of intermediate **4**. These predictions are inconsistent with the observed half-order dependence on [**1b**], nonzero *y*-intercepts for the plots in Figure 1, and direct observation of **4**.

$$\text{rate} = k_{obs}[\mathbf{1b}] \tag{10}$$

$$k_{obs} = \frac{K_1 k_2[\text{P}(t\text{-Bu})_3]}{[\text{P}(o\text{-tol})_3]} \tag{11}$$

Paths D and E, shown in Scheme 5, both describe mechanisms in which reductive elimination of haloarene, with or without an intermediate haloarene complex,[33] is the rate-determining or first irreversible step. This slow reductive elimination from P(*t*-Bu)$_3$-ligated arylpalladium intermediate **4** makes possible the accumulation of **4** during the ligand substitution and reductive elimination sequence. Path D is initiated by associative ligand substitution of P(*t*-Bu)$_3$ for P(*o*-tolyl)$_3$ and reversible cleavage of the dimeric complex to form two P(*t*-Bu)$_3$-ligated arylpalladium(II) halide monomers, **4**. By this mechanism, **4** undergoes reductive elimination of haloarene to form a palladium(0) species that is trapped by P(*t*-Bu)$_3$ to form **2**.

Because **4** accumulates during the reaction, the steady state approximation is inappropriate for the derivation of the rate equations for these mechanisms.

(33) Kulawiec, R. J.; Crabtree, R. H. *Coord. Chem. Rev.* **1990**, *99*, 89.

Thus, preequilibrium methods[34] were used to derive the expressions for k_{obs}. Rate equations for path D are provided in eqs 12−14. The rate expression for k_{obs} includes a term for the concentration of **1b**. This term reflects the change in order in **1b** as a function of the change in concentration of P(*t*-Bu)$_3$. Path D predicts first-order behavior in **1b** when [P(*t*-Bu)$_3$] is large and half-order behavior in **1b** when [P(*t*-Bu)$_3$] is small. It also predicts half-order behavior in **1b** when [**1b**] is high and first-order behavior when [**1b**] is low. This complexity in the order in **1b** may contribute to the similarly close fits of our data to a first-order and a half-order appearance of product. This expression also predicts saturation behavior in P(*t*-Bu)$_3$ and inverse order, saturation behavior in P(*o*-tol)$_3$.

$$\text{rate} = k_{obs}[\mathbf{1b}] \tag{12}$$

$$k_{obs} = \frac{\dfrac{K_1^{1/2}K_2k_3[\text{P}(t\text{-Bu})_3]}{[\text{P}(o\text{-tol})_3][\mathbf{1b}]^{1/2}}}{1 + \dfrac{K_1^{1/2}}{[\mathbf{1b}]^{1/2}} + \dfrac{K_1^{1/2}[\text{P}(t\text{-Bu})_3]}{[\text{P}(o\text{-tol})_3][\mathbf{1b}]^{1/2}}} \tag{13}$$

$$\frac{1}{k_{obs}} = \frac{[\text{P}(o\text{-tol})_3][\mathbf{1b}]^{1/2}}{K_1^{1/2}K_2k_3[\text{P}(t\text{-Bu})_3]} + \frac{[\text{P}(o\text{-tol})_3]}{K_2k_3[\text{P}(t\text{-Bu})_3]} + \frac{1}{k_3} \tag{14}$$

Path E involves reversible or irreversible cleavage of the dimer, followed by exchange of P(*t*-Bu)$_3$ for P(*o*-tolyl)$_3$ and reductive elimination. Again, preequilibrium methods were used to derive rate expressions (eqs 15−17) for this pathway. Like path D, path E predicts saturation behavior in P(*t*-Bu)$_3$ and inverse order, saturation behavior in P(*o*-tolyl)$_3$. It also predicts first-order behavior in **1b** when [P(*t*-Bu)$_3$] is large and half-order behavior in **1b** when [P(*t*-Bu)$_3$] is small.

$$\text{rate} = k_{obs}[\mathbf{1b}] \tag{15}$$

$$k_{obs} = \frac{\dfrac{K_1^{1/2}k_2[\text{P}(t\text{-Bu})_3]}{[\text{P}(o\text{-tol})_3][\mathbf{1b}]^{1/2}}}{1 + \dfrac{K_1^{1/2}[\text{P}(t\text{-Bu})_3]}{[\text{P}(o\text{-tol})_3][\mathbf{1b}]^{1/2}}} \tag{16}$$

$$\frac{1}{k_{obs}} = \frac{[\text{P}(o\text{-tol})_3][\mathbf{1b}]^{1/2}}{K_1^{1/2}k_2[\text{P}(t\text{-Bu})_3]} + \frac{1}{k_2} \tag{17}$$

On the basis of the results and observations above, paths D and E are the most likely mechanisms for the reductive elimination of haloarene from {Pd[P(*o*-tol)$_3$](Ar)(μ-X)}$_2$. These mechanisms fit both the kinetic data and the observation that the monomeric P(*t*-Bu)$_3$-ligated arylpalladium halide intermediate accumulates in observable concentrations during the ligand substitution and reductive elimination processes.

Simulation of Kinetic Data with Dynafit. The complex rate equations for paths D and E in Scheme 5, which included a change in the order of the reaction in **1b** as a function of the relative concentrations of added phosphines and **1b**, made analysis of the kinetic data complex. Dynafit,[35] a data analysis and fitting program, was employed to help evaluate how well the rate equations for paths A−E correlated with our experimental data. The fitting routing was supplied with the mechanistic schemes of paths A−E, data on the concentrations of Pd{P(*t*-Bu)$_3$}$_2$ and LPd(Ar)(Br) versus time, and initial estimated values for the various rate constants associated with each mechanism.

Table 5 contains the rate constants calculated by Dynafit for each of the five possible mechanistic path-

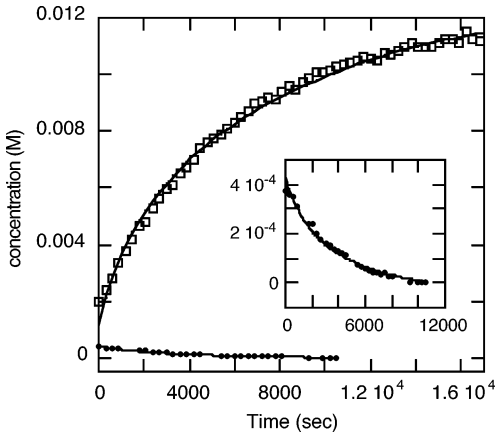

Figure 4. Overlay of data obtained experimentally and profiles for reaction by path D calculated with Dynafit for the reductive elimination of haloarene from **1b**. [Pd(P(*t*-Bu)$_3$)$_2$] (white squares) vs time and [**4**] (black circles) vs time are shown with calculated fits (black lines). Inset contains plot of [**4**] vs time with small *y*-axis range.

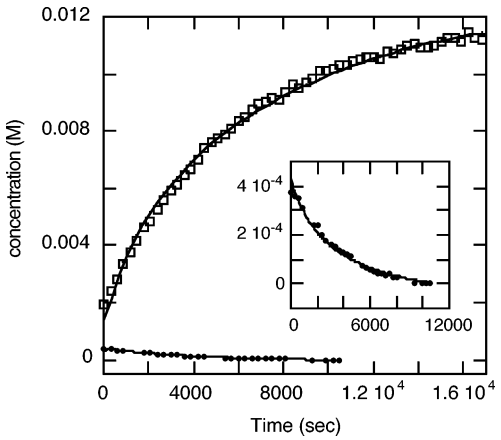

Figure 5. Overlay of data obtained experimentally and profiles for reaction by path E calculated with Dynafit for the reductive elimination of haloarene from **1b**. [Pd(P(*t*-Bu)$_3$)$_2$] (white squares) vs time and [**4**] (black circles) vs time are shown with calculated fits (black lines). Inset contains plot of [**4**] vs time with small *y*-axis range.

Table 5. Values of k_{obs} Generated by Dynafit for Paths A−E

	path A	path B	path C	path D	path E
k_1	8.4×10^{-4}	8.9×10^{6}	4.2×10^{-3}	3.3×10^{-1}	2.7×10^{-3}
k_{-1}	1.3×10^{-1}	2.4×10^{-2}	1.2×10^{-3}	3.4×10^{6}	8.6×10^{2}
k_2	9.3×10^{-3}	1.8×10^{-4}	3.0×10^{-4}	2.0×10^{-3}	6.8
k_{-2}		5.0×10^{1}			3.7×10^{1}
k_3	1×10^{10}	8.9×10^{-1}	1×10^{4}		2.0×10^{-3}
k_4	1×10^{10}		1×10^{4}		

(34) Connors, K. A. *Chemical Kinetics. The Study of Reaction Rates in Solution*; Wiley-VCH: New York, 1990.

(35) Kuzmic, P. *Anal. Biochem.* **1996**, *237*, 260.

ways. Paths A, B, and C are unlikely to be the correct pathways because the rate constants indicate the ligand exchange and dimer cleavage, not reductive elimination, would be rate determining. Moreover, we have shown independently from studies on reductive elimination directly from [P(*t*-Bu)$_3$]Pd(Ar)(Br) that the rate constant for reductive elimination is $(2.0 \pm 0.3) \times 10^{-3}$ $M^{1/2}$ s^{-1}.[20] This value is far from the value obtained for this step from fits to paths A−C.

In contrast, the curves generated by Dynafit that correspond to the mechanisms described by paths D and E agreed well with the experimental data, as seen in Figures 4 and 5. The values of the rate constants for reductive elimination of haloarene were the smallest rate constants generated for both pathways by the fitting routine. Hence, the most likely mechanism for the reductive elimination of haloarene from {Pd[P(*o*-tolyl)$_3$](Ar)(Br)}$_2$ complexes consists of cleavage of the dimer by an associative or dissociative pathway to form intermediate **4**. By either path D or E, this monomer then undergoes reductive elimination of haloarene in the rate-determining step of the process. A good fit to the experimental data was obtained with the rate constant for reductive elimination set to the value measured independently from studies of [P(*t*-Bu)$_3$]Pd(Ar)(Br).[20]

Conclusions

Reductive elimination is often faster from complexes ligated by weakly electron-donating ligands.[21] Electron-withdrawing ligands reduce the electron density on the metal, creating a larger driving force for reduction. However, reductive elimination is induced in the current work by coordination of a strongly electron-donating ligand. Thus, the large steric requirements of P(*t*-Bu)$_3$ (cone angle = 182°) override the electronic effects and induce this unusual type of reductive elimination.[25] For comparison, no reductive elimination of haloarene was observed upon the addition of PCy$_3$ (cone angle = 170°), and only 10−15% yield of haloarene was produced from addition of PCy(*t*-Bu)$_2$ to bromide dimer **1b**. Thus, severe steric crowding can not only accelerate the rate for reductive elimination but alter the thermodynamics so severely that reductive elimination of haloarene is favored thermodynamically.

Experimental Section

General Methods. All manipulations were conducted in an inert atmosphere drybox unless otherwise noted. $^{31}P\{^1H\}$ NMR spectra were recorded on a GE Omega 300 NMR spectrometer. Chemical shifts are referenced to 85% H_3PO_4 as an external standard. ^1H NMR spectra were recorded on a GE QE+ 300 or Bruker 400 NMR spectrometer, and chemical shifts are referenced to tetramethylsilane. All solvents were dried under sodium/benzophenone and distilled under N_2 into an airtight container. Compounds **1d** and **1e** were prepared by literature procedures.[27]

Synthesis of {Pd[P(*o*-tol)$_3$](2-Me-5-*t*-Bu-C$_6$H$_3$)(*μ*-Cl)}$_2$ (1a). A solution of 300 mg (0.235 mmol) of {Pd[P(*o*-tol)$_3$](2-Me-5-*t*-Bu-C$_6$H$_3$)(*μ*-Br)}$_2$ in 5 mL of THF was added to a solution of 255 mg (1.00 mmol) of AgOTf in 5 mL of THF. A fluffy, gray precipitate formed immediately upon mixing. The reaction vessel was wrapped in aluminum foil, and the suspension was allowed to stir for 5 min. The yellow solution was decanted from the precipitate, an additional 5 mL of THF was added to the precipitate, and the new suspension was allowed to stir for 5 min. The yellow solution was again decanted from the precipitate, and the combined 15 mL of decanted solution was filtered through Celite. To the clear yellow solution was added 900 mg (12.1 mmol) of dried KCl. The resulting suspension was allowed to stir for 12 h at room temperature. Once the reaction was complete, as indicated by $^{31}P\{^1H\}$ NMR spectroscopy, the solution was filtered through Celite and then concentrated. Pentane was added to precipitate the product, and the pale yellow solid was filtered, washed with pentane, and dried under vacuum to give 204 mg (73%) of analytically pure product. ^1H NMR (C_7D_8, 105 °C, two isomers): δ 7.8 (br s, 3H), 6.75−7.05 (m, 10H), 6.50−6.75 (m, 2H), 3.04 and 2.88 (br s for two isomers of 5-*t*-Bu-2-*Me*C$_6$H$_3$, 3H), 2.21 (br s, 9H), 0.96 and 0.95 (s for two isomers of *t*-Bu, 9H). $^{31}P\{^1H\}$ NMR (CD_2Cl_2, 25 °C): δ 31.5 (br s). Anal. Calcd for $C_{64}H_{72}P_2Cl_2Pd_2$: C, 64.75; H, 6.13. Found: C, 65.01; H, 5.93.

Synthesis of {Pd[P(*o*-tolyl)$_3$](2-Me-5-*t*-Bu-C$_6$H$_3$)(*μ*-Br)}$_2$ (1b). A solution of 500 mg (0.699 mmol) of Pd[P(*o*-toyl)$_3$]$_2$ in 15 mL of benzene was added to a solution of 410 mg (1.80 mmol) of 2-bromo-1-methyl-4-*tert*-butylbenzene in 5 mL of benzene. Another 80 mL of benzene was added to the reaction vessel to bring the total volume to 100 mL. After 20 min of stirring, the cloudy yellow-green solution was filtered through Celite to remove insoluble material originally present in Pd[P(*o*-tolyl)$_3$]$_2$, and the resulting clear yellow solution was returned to the reaction vessel and allowed to stir for another 4.5 h. When the reaction was complete, as indicated by $^{31}P\{^1H\}$ NMR spectroscopy, the solution was concentrated in vacuo. Pentane was added to the remaining solution to precipitate the product. The yellow solid was filtered, washed with pentane, and dried under vacuum to give 383 mg (86%) of analytically pure product. ^1H NMR (C_7D_8, 105 °C, two isomers): δ 7.8 (br s, 3H), 6.70−7.05 (m, 10H), 6.62 (d, J = 8.1 Hz, 1H), 6.58 (d, J = 7.3 Hz, 1H), 3.09 and 2.87 (br s for two isomers of 5-*t*-Bu-2-*Me*C$_6$H$_3$, 3H), 2.3 (br s, 9H), 0.94 and 0.95 (s for two isomers of *t*-Bu, 9H). $^{31}P\{^1H\}$ NMR (C_6D_6, 25 °C): δ 31.9 (s), 31.1 (br s). Anal. Calcd for $C_{64}H_{72}P_2Br_2Pd_2$: C, 60.23; H, 5.70. Found: C, 59.83; H, 5.72.

Synthesis of {Pd[P(*o*-tolyl)$_3$](2-Me-5-*t*-Bu-C$_6$H$_3$)(*μ*-I)}$_2$ (1c). A procedure similar to that used to prepare **1b** was followed, and the tan product was isolated after precipitation in 70% yield. ^1H NMR (C_7D_8, 105 °C, two isomers): δ 9.1 (br s, 1H), 6.70−7.05 (m, 12H), 6.64 (s, 2H), 3.07 and 2.87 (br s for two isomers of 5-*t*-Bu-2-MeC$_6$H$_3$, 3H), 2.37 (s, 9H), 0.97 (s, 9H). $^{31}P\{^1H\}$ NMR (C_7D_8, 25 °C): δ 28.5 (s), 27.5 (s), 26.8 (s). Anal. Calcd for $C_{64}H_{72}P_2I_2Pd_2$: C, 56.11; H, 5.31. Found: C, 56.11; H, 5.11.

Synthesis of Pd(PPh$_3$)$_2$(4-*t*-BuC$_6$H$_4$)(Br). A solution of 151 mg (0.121 mmol) of {Pd[P(*o*-tolyl)$_3$](4-*t*-BuC$_6$H$_4$)(*μ*-Br)}$_2$ in 5 mL of THF was added to a solution of 133 mg (0.507 mmol) of PPh$_3$ in 5 mL of THF. The color of the solution changed from bright yellow to pale yellow immediately. After 5 min, the reaction was complete, as determined by $^{31}P\{^1H\}$ NMR spectroscopy. The solution was filtered through Celite and concentrated. Pentane was added to precipitate the product as a white solid in 77% yield. The product was filtered, washed with pentane, and dried under vacuum. ^1H NMR (C_6D_6): δ 7.75 (m, 12H), 6.98 (m, 18H), 6.76 (d, J = 8.0 Hz, 2H), 6.31 (d, J = 8.0 Hz, 2H), 1.11 (s, 9H). ^{13}C NMR (CD_2Cl_2): δ 151.6 (t, J = 15.6 Hz), 144.9 (s), 135.6 (t, J = 18 Hz), 135.1 (t, J = 28 Hz), 132.0 (t, J = 89.6 Hz), 130.1 (s), 128.1 (t, J = 16.8 Hz), 125.4 (s), 33.9 (s), 31.7 (s). $^{31}P\{^1H\}$ NMR (C_6D_6): δ 24.5 (s). Anal. Calcd for $C_{46}H_{44}P_2BrPd$: C, 65.45; H, 5.14. Found: C, 65.47; H, 5.41.

Synthesis of Pd(PPh$_3$)$_2$(2-Me-5-*t*-BuC$_6$H$_3$)(Cl) (5a). The same procedure used to synthesize Pd(PPh$_3$)$_2$(4-*t*-BuC$_6$H$_4$)(Br) was followed with a solution of 148 mg (0.125 mmol) of {Pd[P(*o*-tol)$_3$](2-Me-5-*t*-BuC$_6$H$_3$)(*μ*-Cl)}$_2$ in 5 mL of THF and a solution of 139 mg (0.532 mmol) of PPh$_3$ in 5 mL of THF. The reaction produced a 72% yield of analytically pure product.

^{1}H NMR (C_6D_6): δ 7.72 (m, 12H), 6.99 (m, 20H), 6.61 (d, J = 7.8 Hz, 1H), 6.33 (d, J = 8.1 Hz, 1H), 2.07 (s, 3H), 0.94 (s, 9H). ^{13}C NMR (CD_2Cl_2): δ 153.7 (t, J = 15.6 Hz), 146.4 (s), 138.6 (t, J = 15.2 Hz), 135.0 (t, J = 26.4 Hz), 132.4 (t, J = 18 Hz), 131.5 (t, J = 88.4 Hz), 130.3 (s), 130.1 (s), 130.0 (s), 128.1 (t, J = 23.6 Hz), 120.0 (s), 33.7 (s), 31.1 (s), 25.3 (t, J = 28.4 Hz). ^{31}P{^{1}H} NMR (C_6D_6): δ 24.2 (s). Anal. Calcd for $C_{47}H_{46}P_2ClPd$: C, 69.37; H, 5.71. Found: C, 69.53; H, 5.69.

Synthesis of Pd(PPh$_3$)$_2$(2-Me-5-*t*-BuC$_6$H$_3$)(Br) (6b). The same procedure used to synthesize Pd(PPh$_3$)$_2$(4-*t*-BuC$_6$H$_4$)(Br) was followed with a solution of 125 mg (0.0977 mmol) of {Pd[P(*o*-tol)$_3$](2-Me-5-*t*-BuC$_6$H$_3$)(μ-Br)}$_2$ in 5 mL of THF and a solution of 108 mg (0.413 mmol) of PPh$_3$ in 5 mL of THF. This reaction produced a 73% yield of analytically pure product. ^{1}H NMR (C_6D_6): δ 7.72 (m, 12H), 6.98 (m, 18H), 6.60 (d, J = 7.8 Hz, 2H), 6.32 (d, J = 7.8 Hz, 2H), 2.06 (s, 3H), 0.95 (s, 9H). ^{13}C NMR (CD_2Cl_2): δ 155.5 (t, J = 12.8 Hz), 146.5 (s), 138.5 (t, J = 16.4 Hz), 135.0 (t, J = 15.2 Hz), 132.3 (t, J = 22.8 Hz), 131.8 (t, J = 88.4 Hz), 130.3 (s), 130.1 (s), 128.0 (t, J = 16.4 Hz), 120.1 (s), 33.7 (s), 31.1 (s), 25.1 (t, J = 11.2 Hz). ^{31}P{^{1}H} NMR (C_6D_6): δ 24.1 (s). Anal. Calcd for $C_{47}H_{46}P_2BrPd$: C, 65.78; H, 5.30. Found: C, 65.81; H, 5.51.

Measurement of Rate Constant for Reductive Elimination of Haloarene from Arylpalladium(II) Halide Dimers: Representative Procedure. First, 8.1 mg (0.0064 mmol) of {Pd[P(*o*-tol)$_3$](2-Me-5-*t*-Bu-C$_6$H$_3$)(μ-Br)}$_2$ was placed into a small vial and dissolved in 0.42 mL of C_6D_6. Next, 0.10 mL (0.096 mmol) of a 0.96 M solution of P(*t*-Bu)$_3$ in C_6D_6 was syringed into the vial, followed by 0.043 mL (0.032 mmol) of a 0.74 M solution of P(*o*-tolyl)$_3$ in C_6D_6 and 0.057 mL (0.013 mmol) of a 0.22 M solution of 1,3,5-trimethoxybenzene in C_6D_6. This solution was transferred to a septum-lined, screw-capped NMR tube. The sample was put into a GE Omega 300 NMR and heated to 55 °C, and ^{1}H NMR spectra were obtained every 5 min over the course of approximately 8 h.

Determination of Equilibrium Constants for the Reductive Elimination of Haloarene from Arylpalladium Halide Dimers: Representative Procedure. First the equilibrium constant was determined for reductive elimination of haloarene. A sample was prepared by dissolving 8.0 mg (0.0063 mmol) of {Pd[P(*o*-tolyl)$_3$](2-Me-5-*t*-Bu-C$_6$H$_3$)(μ-Br)}$_2$, 2.1 mg (0.012 mmol) of 1,3,5-trimethoxybenzene, and 11.5 mg (0.0568 mmol) of P(*t*-Bu)$_3$ in 0.66 mL of C_6D_6. The solution was mixed and transferred to a septum-lined, screw-capped NMR tube. The sample was heated at 70 °C, and ^{31}P{^{1}H} NMR spectra were obtained periodically until the ratios of the integrations of {Pd[P(*o*-tolyl)$_3$](2-Me-5-*t*-Bu-C$_6$H$_3$)(μ-Br)}$_2$ and Pd[P(*t*-Bu)$_3$]$_2$ remained constant. Final ^{1}H NMR and ^{31}P{^{1}H} spectra were obtained. A single scan was used to obtain ^{1}H NMR spectra, and a pulse delay of 8.7 s (or 5·T_1) was used when obtaining ^{31}P{^{1}H} NMR spectra to ensure full relaxation. Concentrations of all species were calculated and a K_{eq} value was determined from these concentrations.

To obtain K_{eq} from the reverse direction, a sample was prepared by dissolving Pd[P(*t*-Bu)$_3$]$_2$, P(*t*-Bu)$_3$, P(*o*-tolyl)$_3$, 2-Me-5-*t*-Bu-bromobenzene, and 1,3,5-trimethoxybenzene in 0.66 mL of C_6D_6. The data acquisition procedure was the same as that for the reaction run in the forward direction. The value for K_{eq} was within 10% of that for the above measurement.

Acknowledgment. We thank the NIH-NIGMS (GM55382) for support of this work, Johnson-Matthey for a gift of $PdCl_2$, and Merck Research Laboratories for unrestricted support of our program.

OM034277U